Multiagent-based Nonlinear Generalized Minimum Variance Control for Islanded AC Microgrids

Seyed Iman Habibi, Mohammad Amin Sheikhi, Tohid Khalili, *Student Member, IEEE*, Seyyed Ali Ghorashi Khalil Abadi, *Student Member, IEEE*, Ali Bidram, *Senior Member, IEEE*, Josep M. Guerrero, *Fellow Member, IEEE*

Abstract—Voltage regulation, frequency restoration, and reactive/active power sharing are the crucial tasks of the microgrid's secondary control, especially in the islanding operating mode. Because sensors and communication links in a microgrid are subject to noise, it is of paramount value to design a noise-resilient secondary voltage and frequency control. This paper proposes a minimum variance control approach for the secondary control of AC microgrids that can effectively perform noise attenuation, voltage/frequency restoration, and reactive/active power sharing. To this end, the nonlinear generalized minimum variance (NGMV) control approach is introduced to the islanded microgrid's secondary control system. The effectiveness of the proposed control approach is verified by simulating two microgrid test systems in MATLAB.

Index Terms—Microgrid, Secondary Control, Nonlinear Generalized Minimum Variance, Volterra Model .

I. Introduction

microgrid is a small-scale electric power system that effectively integrates distributed generators (DGs) in general and renewable energy sources (RES), e.g., photovoltaic systems, in particular. A reliable, resilient, and efficient microgrid requires an accurately designed control system to accommodate voltage regulation and frequency restoration. Especially after islanding, voltage and frequency controls of a microgrid are more challenging because the microgrid loses its support from the upstream grid. To achieve these control objectives and provide a smooth transition from the grid-connected mode to the islanding mode, microgrids utilize a hierarchical control structure, which involves three levels of control, namely, primary, secondary, and tertiary control levels [1]–[4].

After entering the islanded mode, intentionally or unintentionally, the microgrid's primary control provides the required voltage and frequency stability through the droop control method. However, primary control may result in a slight deviation in the microgrid's voltage and frequency from their nominal values. Secondary control is applied to compensate for those deviations and restore the voltage and frequency of the microgrid to their nominal values [5], [6]. Conventionally, a central controller is used to implement the secondary controller which raises reliability concerns. Recently, distributed control has been introduced to reduce the communication bandwidth and increase the reliability and flexibility of a microgrid [7]–[10]. In a distributed multiagent control framework, each DG is considered as one agent which can communicate with

This material is based upon work supported by the National Science Foundation under Awards OIA-1757207 and ECCS-2214441.

other agents via a communication network. Each agent has only access to its own information and the information of its neighbors [11]-[15].

In practice, measurement noise (e.g., sensors), environmental noise (e.g., rain), and communication noise, (e.g., antenna) are inherent parts of industrial environments [16]-[18]. Especially, in the microgrid distributed control system, the communication noise can act as an additive noise that is either generated at the receiver front end or is the surrounding noise captured by the antennas in the wireless communication. The communication noise can be also categorized as a thermal noise created by the electronic devices and amplifiers at the receivers. The communication noise is commonly modeled by a white noise using a Gaussian distribution model of zero mean and a specific variance value [19]. A Gaussian communication noise with a small variance can impact electronic loads and reduce the longevity of the equipment in long term. On the other hand, a Gaussian noise with a large variance can result in circulating currents in the microgrid and endanger its stability according to [19], [20]. Communication noise can create noise on the control signals like voltage and frequency droop reference values which in turn can have negative impacts on the performance of the secondary control system. Noise on voltage droop reference signal can affect the parameter tuning of proportional-integral (PI) controllers in the internal voltage and current control loops of inverters. Moreover, this noise may have an impact on the switching signals created by the inverter's Pulse Width Modulation (PWM) modules. Noise on the frequency droop reference signal will create an oscillating operating switching frequency for the inverter bridge. Therefore, a noise resilient control approach is required to mitigate the impact of noise in the microgrid control system [21]-[26].

Most of the existing secondary control techniques assume a noise-free environment [7], [10], [11], [13]. In [19], partial feedback linearization and mean square protocol is used to tackle noises in a microgrid. However, reactive power sharing is not accommodated in this work. Reference [21] utilizes a signal estimation technique to estimate reference voltage/frequency set points in a noisy environment. Kalman filter theory is used in [20] to introduce a robust stochastic control for an islanded microgrid. Reference [22] uses iterative learning to deal with an uncertain communication link. A distributed estimation approach is used to attenuate the communication noise. In [23], the effect of Gaussian noise is compensated using a corrective control input which is updated at each sample time. Reference [24] introduces

an adaptive controller based on minimum variance identification. The parameters of the introduced controller can be updated online in different conditions. In [25], a distributed noise resilient economic dispatch approach is introduced to handle the communication link. This method is considered a branch of stochastic approximation. Reference [26] introduces a multiagent-based leader-follower distributed controller to synchronize the frequency in the presence of noise disturbance.

This paper presents a minimum variance-based approach to mitigate the impact of noise on the distributed secondary voltage/frequency control and reactive/active power sharing of an islanded AC microgrid [27], [28]. To this end, nonlinear generalized minimum variance (NGMV) control is used to accommodate both synchronization and noise attenuation. The control scheme is derived based on an identified autoregressive second-order Volterra model for the nonlinear model of a microgrid. The Volterra model is linear in parameters that can be estimated from the routine input-output data using conventional least-squares methods. The Volterra model can be specifically helpful in real-world applications where the exact model of the system is not readily available. Volterra series is recognized as a powerful tool in studying general nonlinear systems and can capture significant nonlinear dynamics of the system [29]–[33]. The proposed optimal controller represents the best achievable control performance for a class of nonlinear microgrid systems in the sense of variance. Furthermore, the proposed method is a simple predictive controller with the prediction horizon of time delay. From a practical point of view, this study not only provides a closed-form solution for the secondary control system but also improves its computational efficiency [31], [32], [34]-[39]. The effectiveness of the proposed control approach is verified by simulating two microgrid test systems in MATLAB.

The contributions of this paper are as follows:

- Multiagent NGMV is utilized for an islanded microgrid as a robust solution against communication noises.
- Unlike most of the work in the literature, the proposed NGMV-based controller is applied discretely. This is particularly important when the proposed controller is implemented on a real system.
- The proposed control scheme is based on a second order Volterra model created for the nonlinear model of a microgrid. The Volterra model is a powerful tool in capturing significant nonlinear dynamics of the system. The Volterra model is created based on the input-output data of system and does not require the exact model of system to be readily available.
- Not only mitigating the noise on the DGs' voltage magnitudes and frequencies, the proposed algorithm can also mitigate the noise on the control signals of the DGs.

The rest of the paper is organized as follows: Section II elaborates on the islanded AC microgrids' primary and secondary control. Section III discusses the NGMV control fundamentals. Multiagent NGMV is proposed for an islanded microgrid in Section IV. Simulation results are provided in Section V. Finally, this paper is concluded in Section VI.

II. MICROGRID'S PRELIMINARIES

This section elaborates on the microgrid's dynamical model and its secondary voltage and frequency control level.

A. AC Microgrid Model

The AC microgrid includes inverter-based DGs, AC loads, and the lines interconnecting them. The microgrid is also equipped with a communication network for the implementation of the microgrid's distributed control. The communication network should be connected meaning that it includes at least one directed spanning tree. The block diagram of an inverter-based DG is shown in Fig. 1. As seen, the DG includes a three-phase inverter bridge and a power source on the DC side. The DG's internal control system includes the power, current, and voltage control loops. The nonlinear dynamical model of an inverter-based DG in d-q reference frame can be represented as [7]

$$\begin{cases} \frac{d}{dt}x_i = f_i(x_i) + k_i(x_i)D_i + g_i(x_i)u_i \\ y_i = h_i(x_i) \end{cases}$$
 (1)

where

$$x_{i} = \begin{bmatrix} \delta_{i} & P_{i} & Q_{i} & \phi_{di} & \phi_{qi} & \gamma_{di} & \gamma_{qi} & i_{ldi} \\ i_{lqi} & v_{odi} & v_{oqi} & i_{odi} & i_{oqi} \end{bmatrix}^{T}$$

$$u_{i} = \begin{bmatrix} V_{ni} & \omega_{ni} \end{bmatrix}^{T}$$

$$y_{i} = \begin{bmatrix} \omega_{i} & v_{oi} \end{bmatrix}^{T}$$

$$(2)$$

where δ_i denotes the angle between i^{th} DG reference frame and the common reference frame; P_i and Q_i describe the active and reactive power of DG, respectively. ϕ_{dqi} and γ_{dqi} are the direct and quadrature components of auxiliary state variables defined in the internal voltage and current control loops. v_{odqi} , i_{ldqi} , and i_{odqi} are the direct and quadrature terms of output voltage, filter current, and output current of DG_i , respectively. f_i , k_i , g_i , and h_i and vector D_i are all defined in [8]. v_{oi} and ω_i are the DG's terminal voltage magnitude and operating frequency; V_{ni} and ω_{ni} are the voltage and frequency droop reference values in the primary control level which are discussed in the following.

The microgrid control system consists of primary, secondary, and tertiary control levels. Primary control is to ensure the stability of the microgrid's voltage and frequency after the microgrid is disconnected from the upstream grid and goes to the islanding mode. The primary control is conventionally implemented using the voltage and frequency droop characteristics

$$\begin{cases} v_{oi} = V_{ni} - n_{Qi}Q_i \\ \omega_i = \omega_{ni} - m_{pi}P_i \end{cases}$$
 (3)

where V_{ni} and ω_{ni} denote the voltage and frequency droop reference values; n_{Qi} and m_{pi} are the voltage and frequency droop coefficients. It should be noted that n_{Qi} and m_{pi} are calculated based on the maximum available reactive and active powers of DGs and they should meet

$$\frac{n_{Qj}}{n_{Qi}} = \frac{Q_{i,\text{max}}}{Q_{j,\text{max}}} \quad , \quad \frac{m_{pj}}{m_{pi}} = \frac{P_{i,\text{max}}}{P_{j,\text{max}}} \tag{4}$$

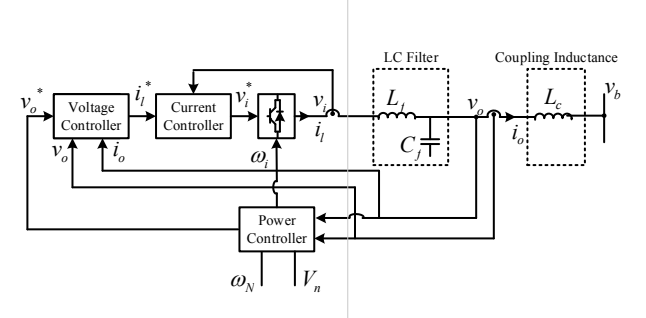


Fig. 1. Voltage-controlled voltage source inverter block diagram.

with $Q_{i,\text{max}}$ and $P_{i,\text{max}}$ as the maximum available reactive and active power at i^{th} DG.

Although the primary control is a vital entity in the microgrid to guarantee voltage and frequency stability, it creates slight voltage and frequency deviations from the nominal voltage and frequency values. These deviations are addressed by the secondary control level which not only synchronizes all DGs' voltage magnitudes and frequencies to the nominal values but also shares the microgrid's reactive and active power among DGs based on their $Q_{i,\max}$ and $P_{i,\max}$ as described in (4). These two goals are addressed by the secondary control level through adjusting V_{ni} and ω_{ni} in (3).

One approach for implementing secondary control is through the distributed control of multiagent systems. Considering each DG as an agent and by differentiating the voltage and frequency droop characteristics, the following dynamical equations can be derived for the secondary control level at each DG

$$\dot{V}_{ni} = \dot{v}_{oi} + n_{Oi}\dot{Q}_i = \alpha_{1i}\dot{v}_{vi} + \beta_{1i}v_{vi} \tag{5}$$

$$\dot{\omega}_{ni} = \dot{\omega}_i + m_{pi}\dot{P}_i = \alpha_{2i}\dot{\omega}_{\omega i} + \beta_{2i}\omega_{\omega i} \tag{6}$$

where $(\alpha_{1iD}, \alpha_{2iD})$ and $(\beta_{1iD}, \beta_{2iD})$ are the proportional and integral coefficients of two discrete-time PI controllers for voltage and frequency control of i^{th} DG, respectively. v_{vi} and $\omega_{\omega i}$ are called the auxiliary control inputs. V_{ni} and ω_{ni} in discrete form can be written as

$$\frac{V_{ni}}{v_{vi}} = \alpha_{1iD} + \frac{\beta_{1iD}T_s}{1 - z^{-1}} \quad , \quad \frac{\omega_{ni}}{\omega_{\omega i}} = \alpha_{2iD} + \frac{\beta_{2iD}T_s}{1 - z^{-1}} \quad (7)$$

where z^{-1} is the backward operation. The control signal is applied at every T_s second.

All DGs can exchange data through a distributed communication network. Therefore, to achieve the above objectives in a distributed fashion, v_{vi} and ω_{vi} are computed as follows,

$$v_{vi} = \sum_{j \in N_i} a_{ij} (v_{oi} - v_{oj}) + g_i (v_{oi} - v_{ref}) + \sum_{j \in N_i} (n_{Qi} Q_i - n_{Qj} Q_j)$$
(8)

$$\omega_{\omega i} = \sum_{j \in N_i} a_{ij} (\omega_i - \omega_j) + g_i (\omega_i - \omega_{nom}) + \sum_{j \in N_i} (m_{pi} P_i - m_{pj} P_j)$$

$$(9)$$

where g_i is the pinning gain that is only nonzero for the master DG that has access to the voltage and frequency reference

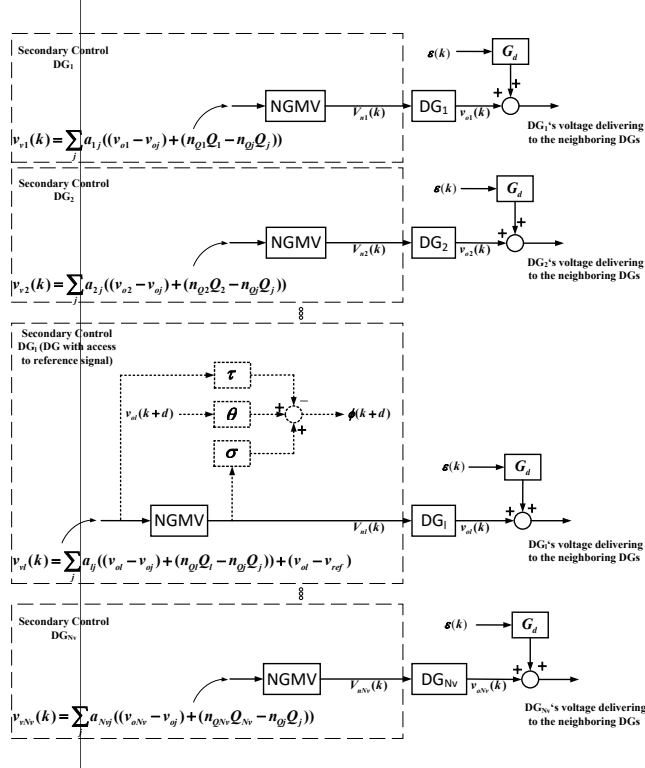


Fig. 2. Multiagent NGMV control structure.

signals (i.e., v_{ref} and ω_{nom}). ω_{nom} is equal to $2\pi f_{nom}$ with f_{nom} denoting the nominal frequency of microgrid.

III. PROPOSED MULTIAGENT NGMV CONTROL

A. Control Architecture and Volterra Model of DGs

The overall architecture of the proposed multiagent NGMV control for the distributed secondary voltage control is illustrated in Fig. 2. As seen, all the conventional controllers described in (7) are replaced with an NGMV controller. It should be noted that a similar architecture is also adopted for the distributed secondary frequency control. In Fig. 2, $\varepsilon(k)$ is the unmeasured stochastic disturbance which can be considered as zero mean white noise; v_{vi} is the local neighborhood tracking error; G_d is the noise dynamic; θ , σ , and τ are dynamic weighting functions, that act as design parameters in the multiagent NGMV controller.

Due to the complexity and nonlinearity of microgrids, using a model that can thoroughly describe the microgrid's dynamic behavior is of particular importance. In this paper, the microgrid is modeled by an autoregressive second-order Volterra model. A Volterra model has the following benefits: (i) The Volterra model is widely used for nonlinear systems without deep knowledge of system dynamics; (ii) despite the nonlinear characteristic of the Volterra model, it takes advantage of being linear in parameters; (iii) it can be identified by conventional least-squares methods [31].

Considering the additive disturbance (noise) $\varepsilon(k)$, one has the following Volterra input-output representation for voltage control on i^{th} DG,

$$T(q^{-1})v_{oi}(k) = h_0 + q^{-d} \left(H_1(q^{-1})V_{ni}(k) + H_2(q_1^{-1}, q_2^{-1})V_{ni}^2(k) \right) + C(q^{-1})\varepsilon(k) ,$$
(10)

where q^{-1} is the backward shift operator and d is the system time delay. The terms h_0 , H_1 , and H_2 correspond to the offset model, and linear and nonlinear term parameters, respectively. The terms $T(q^{-1})$, $H_1(q^{-1})$, $H_2(q^{-1})$, and $C(q^{-1})$ are polynomials of order n_T , n_{H_1} , n_{H_2} , and n_C , respectively. These terms are defined as

$$T(q^{-1}) = \sum_{i=0}^{n_T} a_i q^{-i}, \ a_0 = 1,$$

$$H_1(q^{-1}) = \sum_{i=0}^{n_{H_1}} b_i q^{-i},$$

$$H_2(q_1^{-1}, q_2^{-1}) = \sum_{i=0}^{n_{H_2}} \sum_{j=i}^{n_{H_2}} b_{ij} q_1^{-i} q_2^{-j},$$

$$C(q^{-1}) = \sum_{i=0}^{n_C} c_i q^{-i}, \ c_0 = 1.$$
(11)

$$q^{-1}H_2(q_1^{-1}, q_2^{-1}) \stackrel{\Delta}{=} q_1^{-1}q_2^{-1}H_2(q_1^{-1}, q_2^{-1})$$
 (12)

The disturbance model is,

$$d(k) = G_d(q^{-1})\varepsilon(k) = \frac{C(q^{-1})}{T(q^{-1})}\varepsilon(k)$$
(13)

It should be noted that a similar representation to (10) can be formulated for the frequency control of a DG where instead of v_{oi} and V_{ni} , ω_i and ω_{ni} are used, respectively.

Remark: There is a trade off between the order of model and the computational efficiency of proposed algorithm. for control purposes and practical applications, the common practice is to use less complex but still accurate models to accommodate a reasonable computational burden on the control system. Hence, an appropriate order model with a reasonable computational effort should be selected to calculate the control action within the sampling period. In the identification stage, the estimation problem is a standard regression problem due to the linear in parameters characteristic of Volterra models. Thus, a popular and optimal solution to this problem is the least squares method. Also, we can exploit conventional criteria in the identification context to obtain the orders of polynomials which minimize the estimation error caused by observation errors, unmodeled dynamics, neglected nonlinearities, and unmeasured external disturbances. In this paper, the Normalized Root-Mean-Square Error (NRMSE) criterion is used to find the best-fit model.

B. NGMV Algorithm

The proposed NGMV algorithm aims to reduce the variance of the noise on the DGs' output voltage and operating frequency while synchronizing them to the desired reference voltage and frequency. Herein, the noise is assumed to be a communication noise that affects the voltage and frequency values communicated among DGs. At the same time, this algorithm attenuates the noise on control signals V_{ni} and ω_{ni} in (3) with acceptable variance. In the following the problem is formulated for the secondary voltage control. The same process can be adopted for the secondary frequency control. To this end, the optimal multiagent NGMV control problem can be presented as the minimization of a fictitious signal $\phi(k)$ which is called the generalized output and is expressed as

$$\phi(k+d) = \theta(q^{-1})v_{oi}(k+d) + \sigma(q^{-1})V_{ni}(k) - \tau(q^{-1})v_r(k)$$
(14)

where $v_r(k) = v_{vi}(k) - v_{oi}(k)$. Generalized output $\phi(k+d)$ includes both the system output and the control signal V_{ni} . The terms $\theta = \theta_n/\theta_d$, $\sigma = \sigma_n/\sigma_d$, and $\tau = \tau_n/\tau_d$ are design parameters in the multiagent NGMV controller.

Consider the following Diophantine equation

$$\frac{\theta_n(q^{-1})C(q^{-1})}{\theta_d(q^{-1})T(q^{-1})} = L(q^{-1}) + q^{-d} \frac{F(q^{-1})}{\theta_d(q^{-1})T(q^{-1})}$$
(15)

where L and F are polynomials and have the following forms,

$$L(q^{-1}) = 1 + l_1 q^{-1} + l_2 q^{-1} + \dots + l_{d-1} q^{-(d-1)}$$

$$F(q^{-1}) = f_0 + f_1 q^{-1} + f_2 q^{-1} + \dots + f_{n_f} q^{-n_f}, \qquad (16)$$

$$n_f = \max\{n_C + n_{\theta_n}, n_T + n_{\theta_d} - 1\}$$

By replacing (10) in (14) and employing the Diophantine equation in (15) one has

$$\phi(k+d) = \frac{\theta}{T}h_0 + \frac{\theta H_1}{T}V_{ni}(k) + \frac{\theta H_2}{T}V_{ni}^2(k) + \frac{F}{\theta_d T}\varepsilon(k) + \sigma V_{ni}(k) - \tau v_r(k) + L\varepsilon(k+d)$$
(17)

Considering the model in (10), the noise observer is obtained as

$$\frac{1}{T}\varepsilon(k) = \frac{1}{C}v_{oi}(k) - \frac{1}{CT}h_0 - q^{-d}\frac{H_1}{CT}V_{ni}(k) - q^{-d}\frac{H_2}{CT}V_{ni}^2(k)$$
(18)

Therefore, using observer, (17) can be reformulated as

$$\phi(k+d) = \frac{L}{C} h_0 + \frac{LH_1}{C} V_{ni}(k) + \frac{LH_2}{C} V_{ni}^2(k) + \frac{F}{C\theta_d} v_{oi}(k) + \sigma V_{ni}(k) - \tau v_r(k) + L\varepsilon(k+d)$$
(19)

We define the multiagent NGMV cost function J_{NGMV} in a minimum variance sense such that

$$J_{NGMV} = E\left\{\phi^2\left(k+d\right)|k\right\} \tag{20}$$

where $E\left\{\cdot \left| k \right.\right\}$ denotes the conditional expectation based on measurements up to time k. To find the optimal control solution with respect to minimum variance requirement, cost function (20) needs to break down into two feedback invariant J_{\min} and controller dependent J_0 parts as

$$J_{NGMV} = J_0 + J_{\min}. (21)$$

Consequently, the minimum variance controller tries to make the J_0 term zero. Because the noise sequence information is not available in the future, J_{\min} is independent of any control action. Because of the white noise assumption, future noise values are uncorrelated with their past ones. Hence, the cost function (21) in a separated form can be achieved as

$$J_{NGMV} = E\left\{\phi^2(k+d)|k\right\} = J_0 + J_{\min}$$
 (22)

with

$$J_{0} = E\left\{ \left[\frac{L}{C} h_{0} + \frac{LH_{1}}{C} V_{ni}(k) + \frac{LH_{2}}{C} V_{ni}^{2}(k) + \frac{F}{C\theta_{d}} v_{oi}(k) + \sigma V_{ni}(k) - \tau v_{r}(k) \right]^{2} \right\}$$

$$J_{\min} = E\left\{ \left[L\varepsilon(k+d) \right]^{2} \right\}$$
(23)

The optimal NGMV control law is found by solving the second-degree equation as

$$k_1 V_{ni}^{2}(k) + k_2 V_{ni}(k) + k_3 = 0$$

$$k_1 = \theta_d L H_2, \quad k_2 = \theta_d [L H_1 + C\sigma]$$

$$k_3 = L(1)\theta_d(1)h_0 + F v_{oi}(k) - C\theta_d \tau v_r(k)$$
(24)

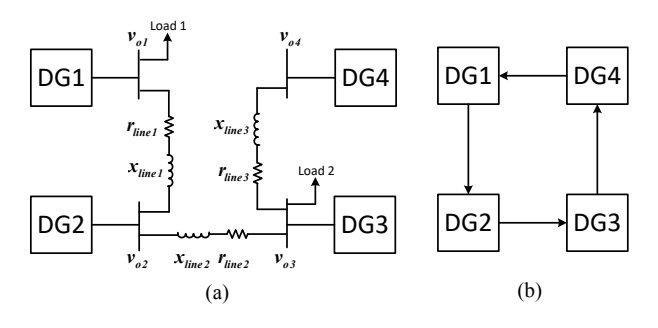


Fig. 3. Microgrid test system I: (a) microgrid single-line diagram; (b) communication graph.

It should be noted that equation (24) might have two solutions in which choosing each of them would depend on control limitations and system. In typical applications, a solution with the smallest absolute value is preferred.

IV. SIMULATION RESULTS

A. Noise Model

The goal of this paper is to tackle the negative impacts of communication noise on the distributed control of AC microgrids. According to [19]–[26]. The communication noise can act as an additive noise that is either generated at the receivers front end or is the surrounding noise absorbed by the antennas in wireless communication. Moreover, the communication noise can be categorized as thermal noise created by the electronic devices and amplifiers at the receivers. The communication noise is commonly modeled by a white noise using a Gaussian distribution model of zero mean and a specific variance value [19]. In this paper, we have selected different variance values to highlight the performance of NGMV algorithms under different Gaussian noise models. The communication noise that is added to the communicated voltage and frequency values as seen in Fig. 2.

B. Case A - Microgrid test system I

The communication graph and the single-line diagram of this microgrid test system are shown in Fig. 3. The parameters of this microgrid are provided in TABLE I. It is assumed that the microgrid goes to islanding mode at t=1 s. DG1 has access to the voltage reference signals (v_{ref}) and the frequency reference signal (ω_{nom}) , respectively. For the microgrid test system I, four proper Volterra models for frequency control and four proper Volterra models for voltage control are identified. The simulations are performed in MATLAB. The control loop is updated at every 1 msec. The parameters of the identified Volterra model for DG1's voltage are provided in TABLE II.

It is assumed that at t=1 s, additive white noises are simulated on the communication links among the DGs affecting the voltage and frequency measurements received at the neighboring DGs. These communication noises are modelled as a Gaussian noise and affect both the transmitted voltage and frequency values at the same time. To verify the effectiveness of our proposed approach under different

TABLE I
THE PARAMETERS OF MICROGRID TEST SYSTEM I.

Value
380 V, 50 Hz
9.4e - 5
[1.3, 1.3, 1.5, 1.5]e - 3
1Ω
1Ω
$5e-2\Omega$
0.5Ω
[0.05, 10.5, 390, 16e3]
[.35 mH, 50 μ F, 0.35 mH]

TABLE II
THE VOLTAGE VOLTERRA MODEL FOR MICROGRID TEST SYSTEM I

	i = 0	i = 1	i = 2
T_i	1	-1.894	0.89
$H_{1,i}$	-2.04e-04	1.89e-04	-
$H_{2,1i}$	-2.74e-07	4.43e-07	-
$H_{2,2i}$	-	-1.73e-07	-
h_0	1.67	-	-

variance values of modelled noise, two different cases studies are simulated. In Case A.1, white noises with variance of 4 are added to the communicated DG voltage measurements while white noises with variance of 0.1 are added to the communicated DG frequencies. In Case A.2, white noises with the variance of 4 are added to both the communicated voltage and frequency values among DGs. The voltage and frequency regulation and active and reactive power sharing are being done simultaneously. In order to verify the performance of the proposed NGMV control, the impact of noise is investigated first on the conventional distributed secondary control. To this end, integral controller $c = \frac{0.02z^{-1}}{1-z^{-1}}$ is adopted for both the secondary frequency and voltage control on all DGs (see (7)). Then, the impact of noise on NGMV controller is studied. The designing parameters of the multiagent NGMV controllers are, $\theta = 0.02$, $\sigma = (0.6 - 0.6z^{-1})$, and $\tau =$ $(0.02 \times 0.98)/(1 - 0.98z^{-1})$. The simulation results for Case A.1 when multiagent NGMV and conventional distributed secondary controls are utilized are provided in Figs. 4, 5, 9, 9, 6 and 8. It should be also noted that the conventional distributed secondary control creates a noticeable amount of noise on the voltage and frequency droop reference signals. However, the multiagent NGMV controller tunes the output by also accounting for the control signal. With a well-designed multiagent NGMV controller, noise can be attenuated in the control signals (i.e., V_n and ω_n) as seen in Figs. 6 and 8. The simulation results for Case A.2 when multiagent NGMV and conventional distributed secondary controls are utilized are provided in Figs. 10 and 11. As seen, the conventional secondary control renders higher noise values on the DGs' terminal voltage magnitudes and frequencies and the proposed NGMV algorithm can effectively mitigate the impact of noise under different varaince values.

In order to show the robustness of the proposed method, the resistances of both loads are changed from 1 Ω to 3 Ω at t=5 s in *Case A.3*. The simulation results when multiagent NGMV

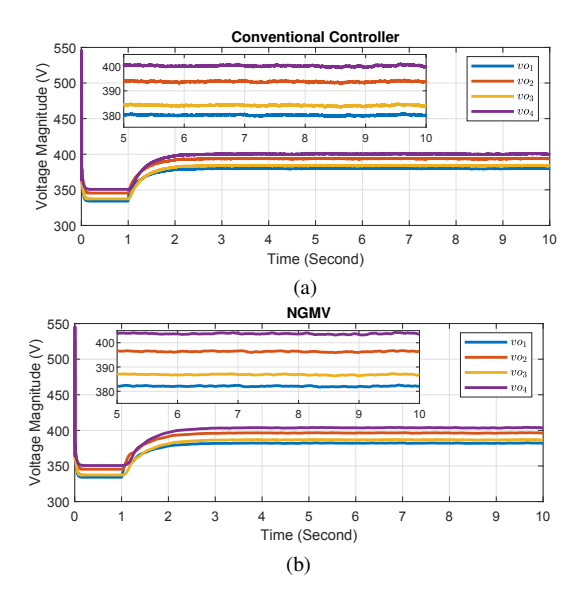


Fig. 4. Case A.1 - Voltage magnitudes of DGs: (a) conventional distributed secondary control; (b) NGMV-based distributed secondary control.

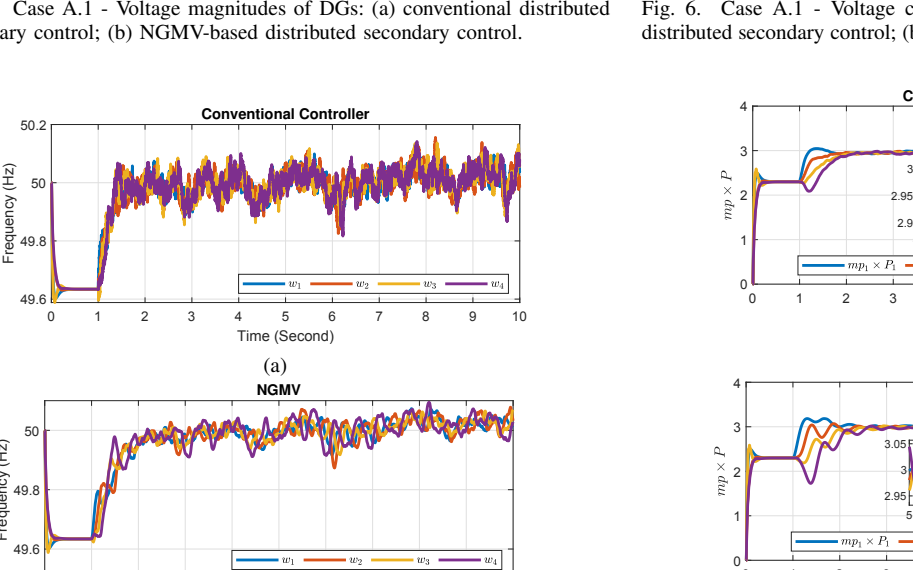


Fig. 5. Case A.1 - Frequencies of DGs: (a) conventional distributed secondary control; (b) NGMV-based distributed secondary control.

Time (Second)

and conventional distributed secondary controls are utilized are provided in Figs. 12 and 13. As seen, the multiagent NGMV is robust with respect to the load changes and can effectively mitigate the impact of noise of both DGs' voltage and frequency.

Microgrid test system I is also simulated for 50 different random noise sequences. The box plots of the noise variances for DGs' voltage magnitudes and frequencies using the proposed multiagent NGMV-based and the conventional secondary controllers are presented in Fig. 14. The central red mark in the box plots is the median. As seen, the voltage magnitude and frequency variances of all the DGs are improved in the proposed NGMV-based distributed secondary control compared to the conventional controller in all 50 simulations using 50 different random noise sequences.

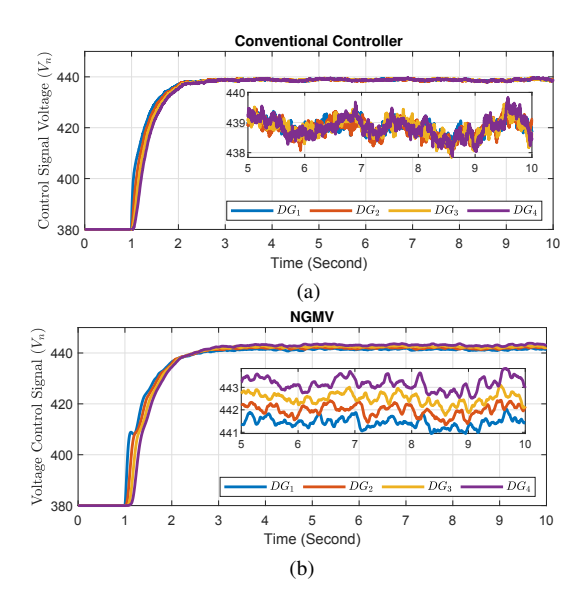


Fig. 6. Case A.1 - Voltage control signal (V_n) of DGs: (a) conventional distributed secondary control; (b) NGMV-based distributed secondary control.

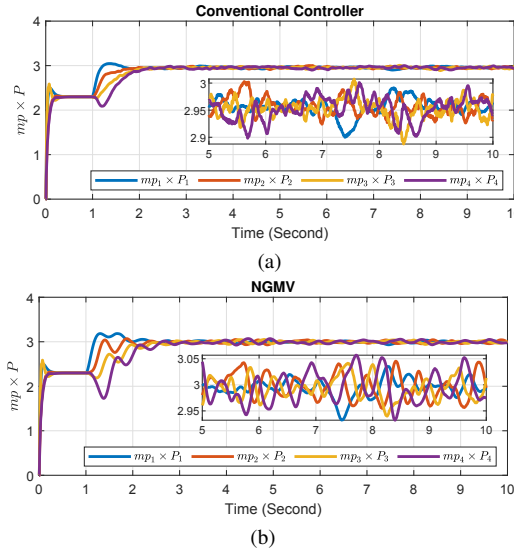


Fig. 7. Case A.1 - Active power ratios of DGs: (a) conventional distributed secondary control; (b) NGMV-based distributed secondary control.

C. Case B - Microgrid test system II

The second microgrid test system with 20 DGs is shown in Fig. 15. The communication graph for this microgrid is illustrated in Fig. 16. The parameters of this microgrid are provided in TABLE III. At t = 0.6 s, the microgrid goes into islanding mode. It is assumed that at t = 0.6 s, additive white noises are simulated on the communication links among the DGs affecting the voltage and frequency measurements received at the neighboring DGs. These communication noises are modelled as a Gaussian noise and affect both the transmitted voltage and frequency values at the same time. DG1 has access to the voltage reference signals (v_{ref}) and the frequency reference signal (ω_{nom}). The voltage and frequency control and reactive and active power sharing are being performed simultaneously. The control loop is updated at every 0.1 second. Forty proper Volterra models for frequency and voltage

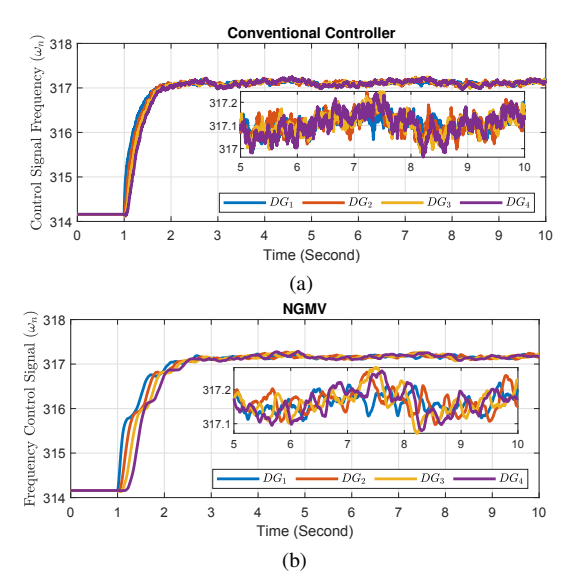


Fig. 8. Case A.1 - Frequency control signal (ω_n) of DGs in Microgrid test system I with voltage and frequency noise variance 4 and 0.1, respectively: (a) conventional distributed secondary control; (b) NGMV-based distributed secondary control.

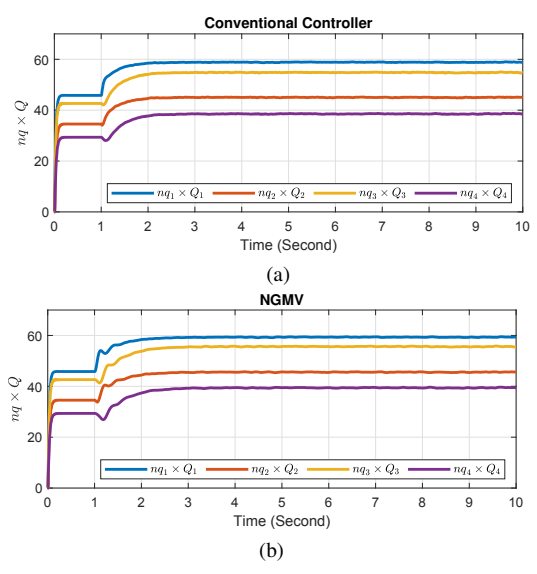


Fig. 9. Case A.1 - Reactive power ratios of DGs in Microgrid test system I with voltage and frequency noise variance 4 and 0.1, respectively: (a) conventional distributed secondary control; (b) NGMV-based distributed secondary control.

controls are identified for this microgrid. The parameters of the voltage Volterra model for DG1 are presented in TABLE IV.

To verify the performance of the proposed NGMV-based distributed secondary control, the results of this method are compared with the conventional distributed secondary control. The design parameters for the multiagent NGMV are $\theta=1$, $\sigma=(5-5z^{-1})/1$, and $\tau=1$. The designed conventional controllers are $c_f=\frac{0.09z^{-1}}{1-z^{-1}}, c_v=\frac{1.1z^{-1}}{1-z^{-1}}$, where c_f and c_v are the conventional controllers for frequency and voltage of the microgrid, respectively. We have utilized two different variance values for the Gaussian noise model, where in *case B.1* variance of 0.09 is utilized for both voltage and frequency

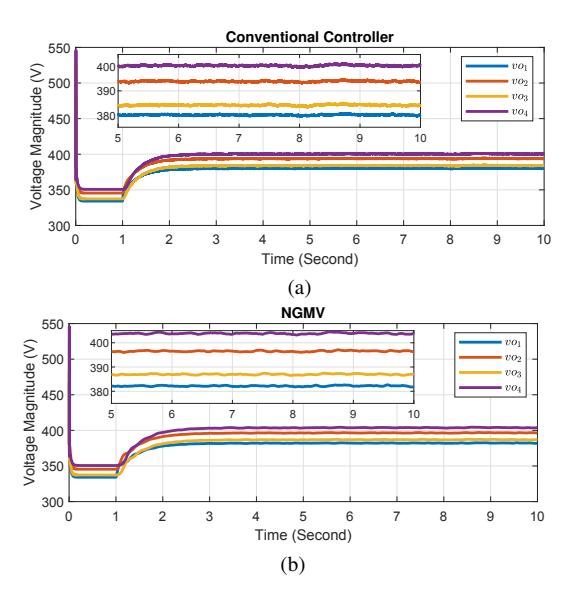


Fig. 10. Case A.2 - Voltage magnitudes of DGs: (a) conventional distributed secondary control; (b) NGMV-based distributed secondary control.

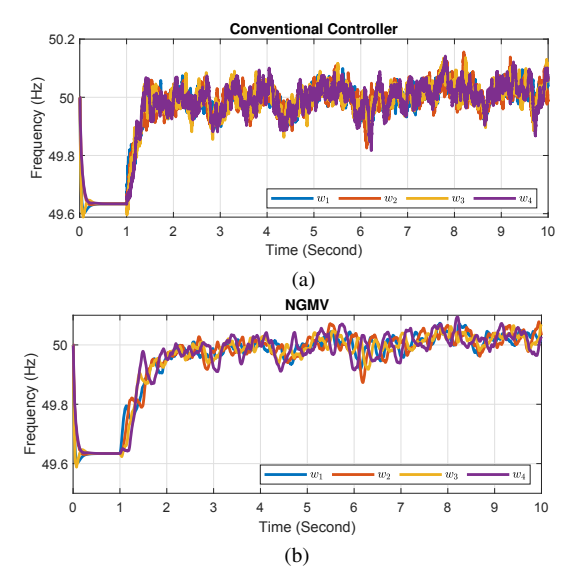


Fig. 11. Case A.2 - Frequencies of DGs: (a) conventional distributed secondary control; (b) NGMV-based distributed secondary control.

and in *Case B.2*, variance of 4 is utilized for both voltage and frequency. For *case B.1*, Figs. 17, 18, 19, 20, 21, and 22 show the results of the proposed multiagent NGMV-based compared to the conventional distributed secondary controllers. As seen, the NGMV-based distributed secondary controller noise attenuation is much better than the conventional controller. For the control signals (i.e., V_n and ω_n), Figs. 21 and 22 show that the variance of the control signals in the conventional controller is much higher than the variance of the control signal in the proposed multiagent NGMV. For *case B.2*, Figs. 23 and 24 show that NGMV-based control can effectively work with a higher noise variance value.

The microgrid test system II is simulated for 50 different random noise sequences. The box plots of the noise variances for DGs' voltage magnitudes and frequencies are reported in Fig. 25-32. As seen, the multiagent NGMV-based distributed

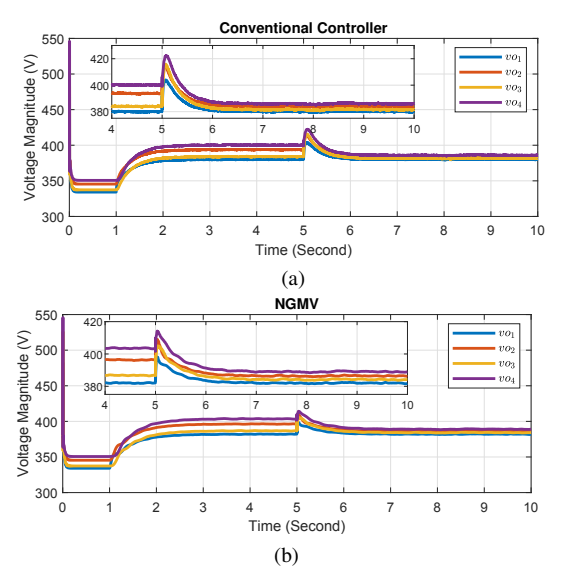


Fig. 12. Case A.3 - Voltage magnitudes of DGs in Microgrid test system I with voltage and frequency noise variance 4 and the loads' resistance are changed from 1 Ω to 3 Ω : (a) conventional distributed secondary control; (b) NGMV-based distributed secondary control.

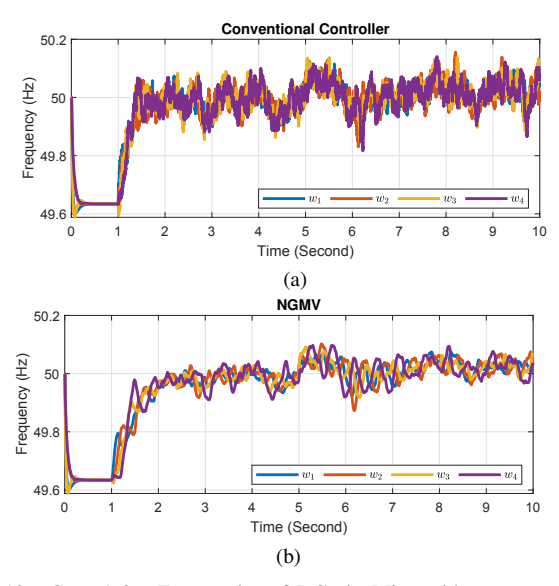


Fig. 13. Case A.3 - Frequencies of DGs in Microgrid test system I with voltage and frequency noise variance 4 and the loads' resistance are changed from 1 Ω to 3 Ω : (a) conventional distributed secondary control; (b) NGMV-based distributed secondary control.

secondary control renders a better performance in attenuating the added noise in the voltage magnitudes and frequencies.

V. CONCLUSION

This paper proposes a minimum variance control approach for the voltage and frequency secondary control of inverter-based AC microgrids in the presence of noise. To this end, a multiagent NGMV control is introduced for the microgrid's distributed control system. Multiagent NGMV aims to minimize a cost function including the output, control signal, and reference signal. This method results in a comparably smooth signal in the microgrid which can increase the reliability and decrease the maintenance cost of a microgrid. Two microgrid

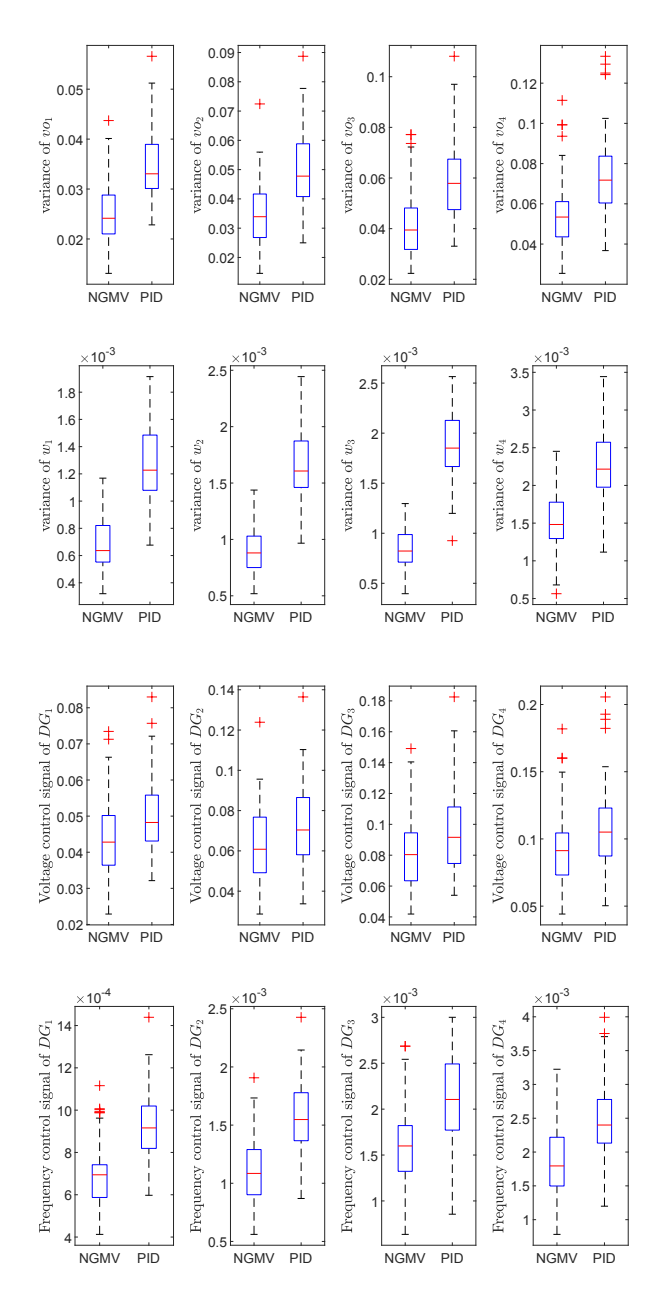


Fig. 14. Comparison of the variance of noise on DGs' voltage magnitudes and frequencies in Microgrid test system I for 50 different noise sequences.

test systems are simulated in MATLAB to verify the effectiveness of the proposed method. 50 different noise sequences are generated in both test systems. The mean of the variance of all signals for the conventional and the proposed multiagent NGMV are reported and compared in this paper.

APPENDIX A PRELIMINARIES OF GRAPH THEORY

The communication system used in the proposed distributed secondary control can be modelled using a graph. A graph is specified through a set of nodes and edges, i.e., $\varsigma=(v,\varepsilon,\mathrm{A})$, where v denotes a finite set of Nv nodes that are connected to each other through edges $\varepsilon\subset v\times v$. The connection of nodes

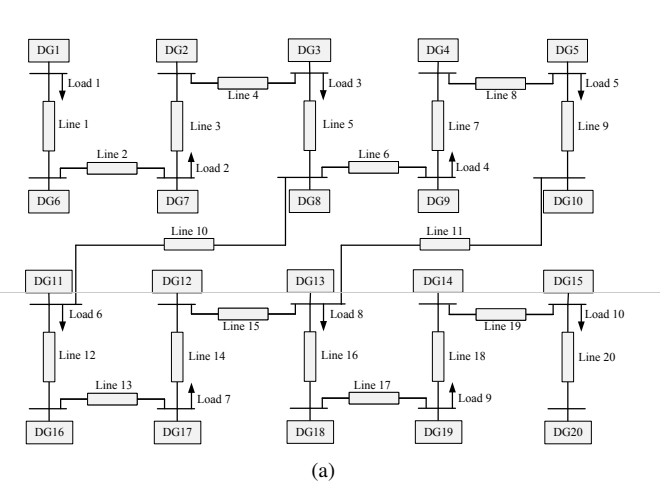


Fig. 15. Microgrid test system II: Communication graph

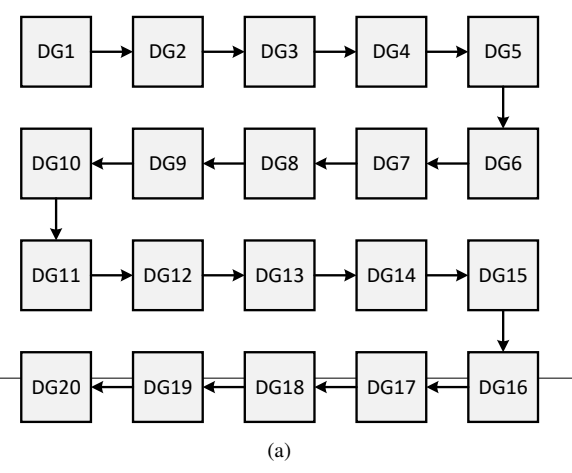


Fig. 16. Microgrid test system II: A microgrid with 20 DGs.

can be described using adjacency matrix A with $A = [a_{ij}] \in R^{Nv \times Nv}$. a_{ij} shows the weight of the edge (v_j, v_i) . If node i is the receiver of data from node j, then node j is called a neighbor of the node i and $(v_j, v_i) \in \varepsilon$. $N_i = \{j | (v_j, v_i) \in \varepsilon\}$ is a set that defines the neighbors of node i [7].

APPENDIX B ROBUSTNESS AND STABILITY ANALYSIS

On the robustness: In our design, the effect of unavoidable plant/model mismatch, disturbances of known and unknown sources is considered as an additive disturbance model that affects the system. The proposed control scheme try to deal with plant/model mismatch, and eliminates all deviation from target by minimizing the expected squared deviation of system output from its desired target value. Another tool we can employ in this proposed control scheme, is utilizing the dynamic weighting functions to attenuate the plant/model mismatch. For instance, considering an integrating term in the designing parameters leads to an offset-free scheme as we did in the whole manuscript's simulation parts. Therefore, there is some robustness to the proposed structure. To address the reviewer's comment, the authors provide a simulation study to verify the assertion. According to the results, the proposed control

TABLE III
THE PARAMETERS OF THE MICROGRID TEST SYSTEM II.

Parameter	Value
v_{nom}, f_{nom}	380 V, 50 Hz
$[m_{p1},,m_{p20}]$	9.4e - 5
$[R_{load1},,R_{load1}]$	1Ω
$[X_{load1},,X_{load1}]$	1Ω
$[n_{Q1}, n_{Q3},, n_{Q19}]$	1.3e - 3
$[n_{Q2}, n_{Q4},, n_{Q20}]$	1.5e - 3
$[r_{line1},,r_{line20}]$	$0.1~\Omega$
$[x_{line1},,x_{line20}]$	0.5Ω
$[K_{pv}, K_{pc}, K_{iv}, K_{ic}]$	[0.05, 10.5, 390, 16e3]
$[L_f, C_f, L_c]$	[1.35] mH, 50 μ F, 0.35 mH]

Voltage Volterra model parameters for DG1 of microgrid test system II.

	i = 0	i = 1	i = 2	i = 3	i = 4
T_i	1	-2.37	2.05	-0.66	0.05
$H_{1,i}$	1.02	-2.48	2.04	-0.55	-
$H_{2,1i}$	-2.86e-04	0.02	0	-0.02	-
$H_{2,2i}$	-	-0.02	0	0.03	-
$H_{2,3i}$	-	-	0.01	0.01	-
$H_{2,4i}$	-	-	-	7.11e-05	-
h_0	15.14	-	-	-	-

has an acceptable performance, and plant uncertainty does not considerably affect the efficiency.

On the stability: The introduced autoregressive Volterra model for the AC Microgrid system is BIBO (bounded-input, bounded-output) stable if the pole locations of the linear autoregressive part of this model $(T(q^{-1}))$ lie inside the unit circle as is shown in [30] and stated as: "The stability of an AR-Volterra model is seen to depend only on the pole locations of linear autoregressive part of this model, and may be determined from the coefficient γ_i by standard results for linear discrete-time models". The system inputs are the voltage and frequency droop reference values and are physically bounded. Hence, closed-loop BIBO stability is guaranteed from the set-point to the output provided the roots of the linear characteristic equation are within the unit circle.

The first Volterra model (Table II):

$$T(q^{-1}) = 1 - 1.894q^{-1} + 0.899q^{-2} \rightarrow$$
roots:
$$\begin{cases} z_1 = 0.9484 \rightarrow |z_1| < 1\\ z_2 = 0.9484 \rightarrow |z_2| < 1 \end{cases}$$
 (25)

The second Volterra model (Table IV):

$$T(q^{-1}) = 1 - 2.37q^{-1} + 2.05q^{-2} - 0.66q^{-3} + 0.05q^{-4} \rightarrow$$

$$coots: \begin{cases} z_1 = 0.9550 \rightarrow |z_1| < 1 \\ z_2 = 0.9550 \rightarrow |z_2| < 1 \\ z_3 = 0.5111 \rightarrow |z_3| < 1 \\ z_4 = 0.1073 \rightarrow |z_4| < 1 \end{cases}$$
(26)

Further, we analyze the optimization problem and the optimal solution.

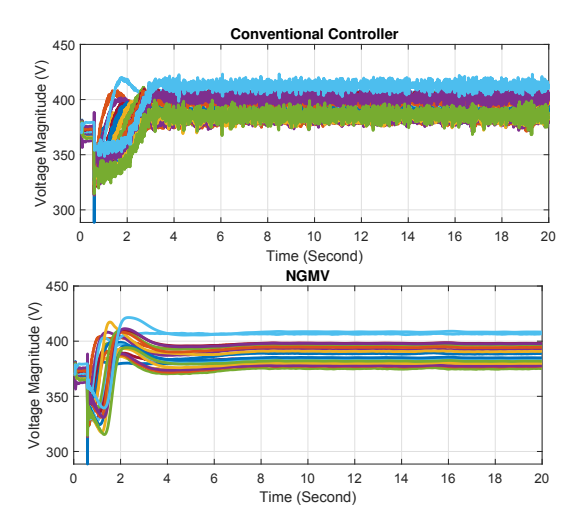


Fig. 17. Case B.1 - Voltage magnitudes of DGs: (a) conventional distributed secondary control; (b) NGMV-based distributed secondary control.

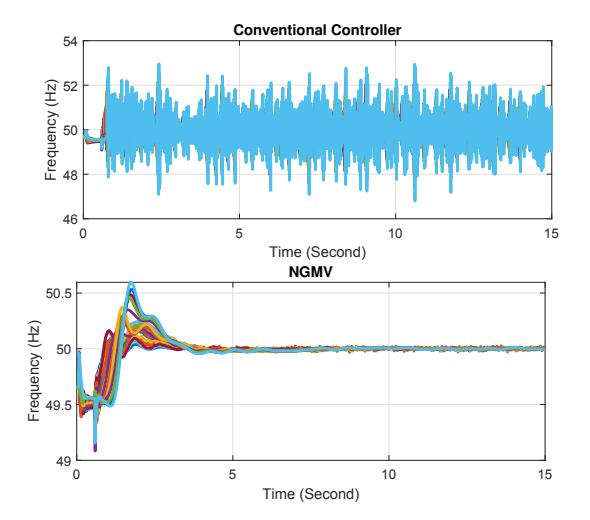


Fig. 18. Case B.1 - Frequency of DGs: (a) conventional distributed secondary control; (b) NGMV-based distributed secondary control.

Definition 1 [40], [41] A function $f:\mathbb{R}^n\to\mathbb{R}$ is convex if and only if, it satisfies

$$\alpha f(x^a) + (1 - \alpha)f(x^b) \ge f(\alpha x^a + (1 - \alpha)x^b) \tag{27}$$

for all $\alpha \in [0,1]$ and all points $x^a, x^b \in \mathbb{R}^n$. So, we have

$$f = \phi^{2} = (\theta v_{oi} + \sigma V_{ni} - \tau v_{r})^{2}$$

= $\sigma^{2} V_{ni}^{2} + 2\sigma (\theta v_{oi} - \tau v_{r}) V_{ni} + (\theta v_{oi} - \tau v_{r})^{2}$ (28)

For simplicity, consider $(\theta v_{oi} - \tau v_r)^2 = \Upsilon$ and rewrite the cost function

$$f = \sigma^2 V_{ni}^2 + 2\sigma(\theta v_{oi} - \tau v_r) V_{ni} + \Upsilon \tag{29}$$

Thus, J_{NGMV} is a standard quadratic form of f(x): $x^TAx + B^Tx + C$. Then, we need to check the convexity condition

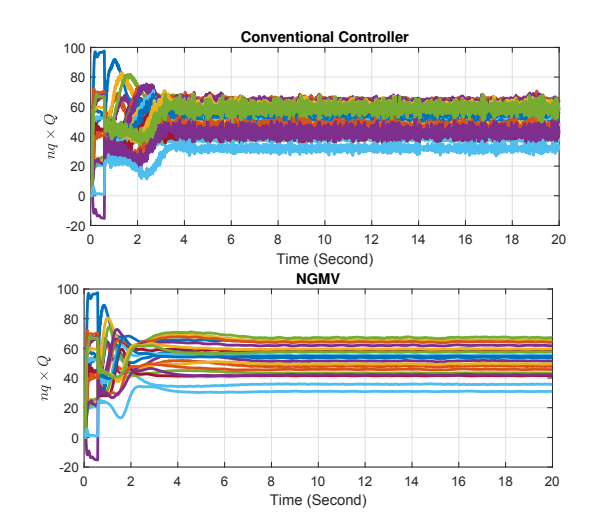


Fig. 19. Case B.1 - Reactive power ratio of DGs: (a) conventional distributed secondary control; (b) NGMV-based distributed secondary control.

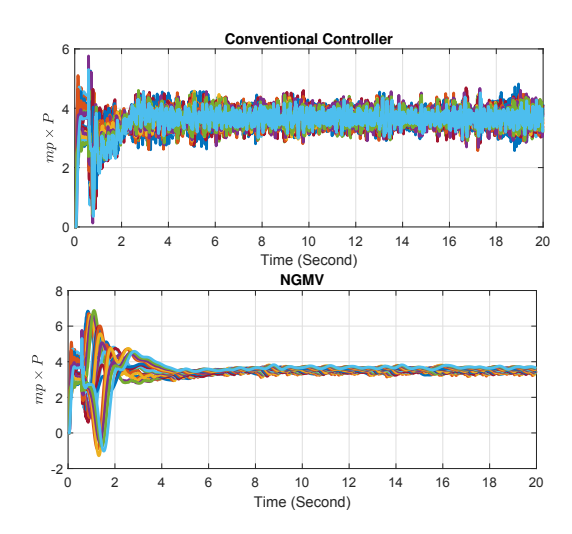


Fig. 20. Case B.1 - Active power ratio of DGs: (a) conventional distributed secondary control; (b) NGMV-based distributed secondary control

provided in **Definition 1**.

$$\alpha \left(\sigma^{2} V_{ni}^{a^{2}} + 2\sigma(\theta v_{oi} - \tau v_{r}) V_{ni}^{a} + \Upsilon\right)$$

$$+ (1 - \alpha) \left(\sigma^{2} V_{ni}^{b^{2}} + 2\sigma(\theta v_{oi} - \tau v_{r}) V_{ni}^{b} + \Upsilon\right) \geq$$

$$\sigma^{2} \left(\alpha V_{ni}^{a} + (1 - \alpha) V_{ni}^{b}\right)^{2}$$

$$+ 2\sigma(\theta v_{oi} - \tau v_{r}) \left(\alpha V_{ni}^{a} + (1 - \alpha) V_{ni}^{b}\right) + \Upsilon$$

$$(30)$$

After some mathematical manipulations and factorizing, we have

$$\alpha(1-\alpha)\sigma^{2}V_{ni}^{a^{2}} + \alpha(1-\alpha)\sigma^{2}V_{ni}^{b^{2}} - 2\alpha(1-\alpha)\sigma^{2}V_{ni}^{a}V_{ni}^{b} \ge 0$$

$$\Rightarrow \alpha(1-\alpha)\sigma^{2}\left(V_{ni}^{a^{2}} + V_{ni}^{b^{2}} - 2V_{ni}^{a}V_{ni}^{b}\right) \ge 0$$
(31)

$$\Rightarrow \alpha (1 - \alpha) \sigma^2 \left(V_{ni}^a - V_{ni}^b \right)^2 \ge 0 \tag{33}$$

As $\alpha(1-\alpha) \geq 0$ (Assumption!), the cost function J_{NGMV} is convex. Therefore, if the second-order equation has a

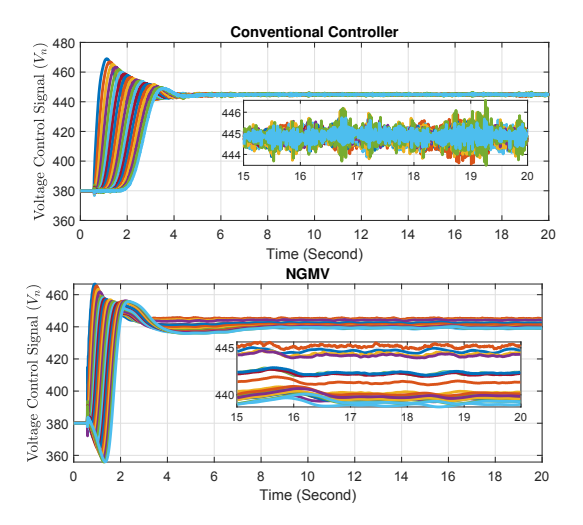


Fig. 21. Case B.1 - Voltage control signal (V_n) of DGs: (a) conventional distributed secondary control; (b) NGMV-based distributed secondary control.

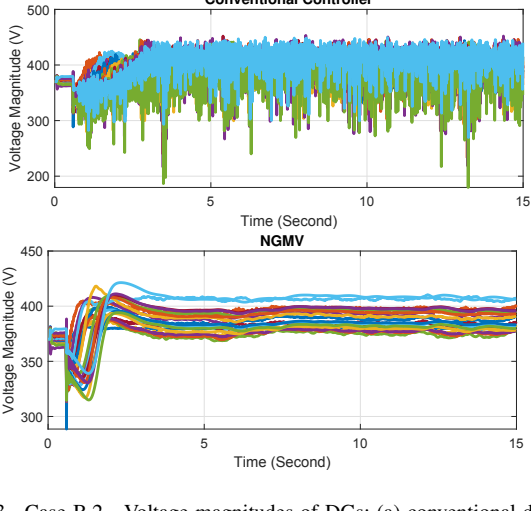


Fig. 23. Case B.2 - Voltage magnitudes of DGs: (a) conventional distributed secondary control; (b) NGMV-based distributed secondary control.

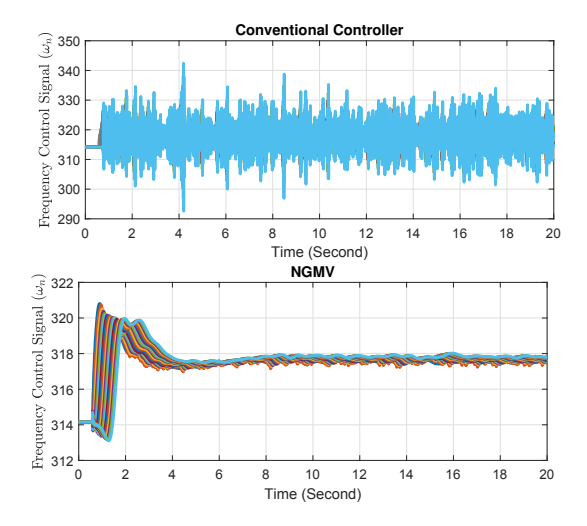


Fig. 22. Case B.1.- Frequency control signal (ω_n) of DGs: (a) conventional distributed secondary control; (b) NGMV-based distributed secondary control.

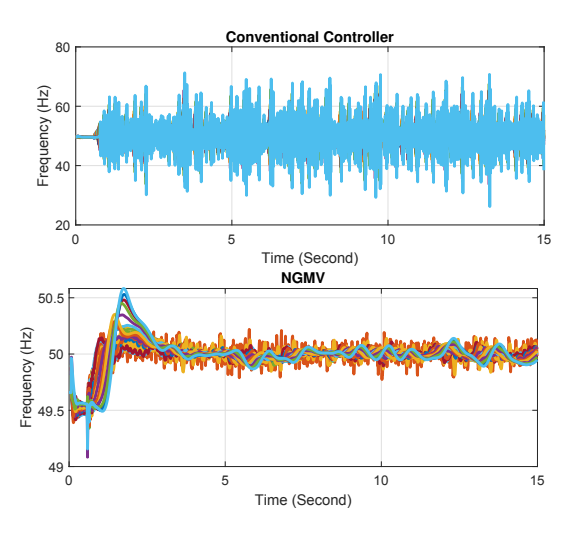


Fig. 24. Case B.2 - Frequency of DGs: (a) conventional distributed secondary control; (b) NGMV-based distributed secondary control.

solution, the closed-loop system after substituting the control signal in Equation (17) of manuscript will be reduced to polynomial term $E\varepsilon(k+d)$, which is bounded. In this case $(\Delta \geq 0 \equiv k_2^2 - 4k_1k_3 \geq 0)$, the bounded control signal provides bounded output. To satisfy bounded control signal condition, it is plentiful to ensure stability of the control law, which is achievable by restricting its poles to be inside the unit circle. According to Equation (24) of manuscript, the dominator of the control law is $\theta_d E H_2$. Therefore, selecting proper stable weightings transfer functions θ such that all eigenvalues of $\theta_d E H_2$ be inside the unit circle ensures stability of the control law as well as the closed-loop system. For the $\Delta < 0$ case, we consider a real value for the control signal in the control scheme, which means the control signal is still bounded. As a result, BIBO stability could be achieved.

REFERENCES

[1] C. Furlan and C. Mortarino, "Forecasting the impact of renewable energies in competition with non-renewable sources," *Renewable and Sustainable Energy Reviews*, vol. 81, pp. 1879–1886, Jan. 2018.

- [2] G. Dileep, "A survey on smart grid technologies and applications," Renewable Energy, vol. 146, pp. 2589–2625, Feb. 2020.
- [3] N. Pogaku, M. Prodanovic, and T. C. Green, "Modeling, analysis and testing of autonomous operation of an inverter-based microgrid," *IEEE Trans. Power Electronics*, vol. 22, no. 2, pp. 613–625, Mar. 2007.
- [4] M. Farrokhabadi, C. A. Cañizares, J. W. Simpson-Porco, E. Nasr, L. Fan, P. A. Mendoza-Araya, R. Tonkoski, U. Tamrakar, N. Hatziargyriou, D. Lagos et al., "Microgrid stability definitions, analysis, and examples," *IEEE Trans. Power Systems*, vol. 35, no. 1, pp. 13–29, Jan. 2020.
- [5] A. Bidram and A. Davoudi, "Hierarchical structure of microgrids control system," *IEEE Trans. Smart Grid*, vol. 3, no. 4, pp. 1963–1976, Dec. 2012.
- [6] J. Lai and X. Lu, "Nonlinear mean-square power sharing control for ac microgrids under distributed event detection," *IEEE Trans. Industrial Informatics*, vol. 17, no. 1, pp. 219–229, Jan. 2021.
- [7] A. Bidram, A. Davoudi, and F. L. Lewis, "A multiobjective distributed control framework for islanded ac microgrids," *IEEE Trans. Industrial Informatics*, vol. 10, no. 3, pp. 1785–1798, Aug. 2014.
- [8] A. Bidram, A. Davoudi, F. L. Lewis, and J. M. Guerrero, "Distributed cooperative secondary control of microgrids using feedback linearization," *IEEE Trans. Power Systems*, vol. 28, no. 3, pp. 3462–3470, Aug. 2013
- [9] S. I. Habibi and A. Bidram, "Unfalsified switching adaptive voltage control for islanded microgrids," *IEEE Trans. Power Systems*, vol. 37, no. 5, pp. 3394–3407, Sept. 2022.
- [10] J. Choi, S. I. Habibi, and A. Bidram, "Distributed finite-time event-

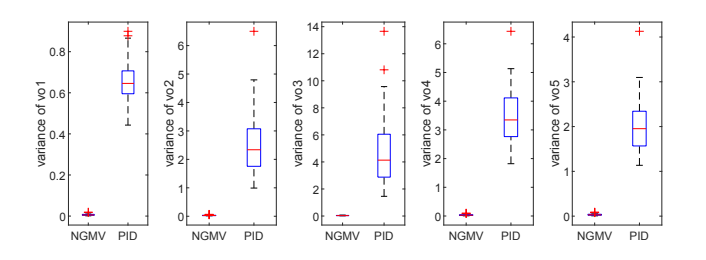


Fig. 25. Comparison of the variance of noise on DG1's to DG5's voltage magnitudes in Microgrid test system II for 50 different noise sequences.

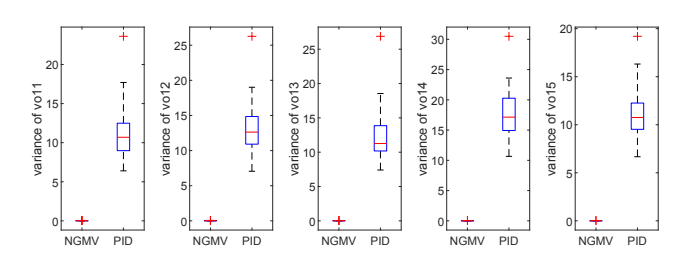


Fig. 27. Comparison of the variance of noise on DG11's to DG15's frequencies in Microgrid test system II for 50 different noise sequences.

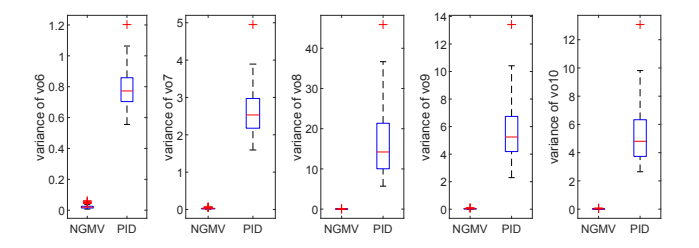


Fig. 26. Comparison of the variance of noise on DG6's to DG10's voltage magnitudes in Microgrid test system II for 50 different noise sequences.

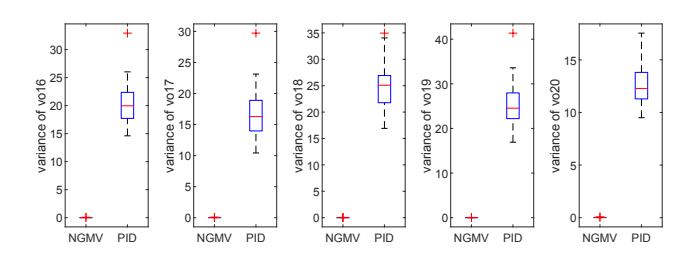


Fig. 28. Comparison of the variance of noise on DG16's to DG20's voltage magnitudes in Microgrid test system II for 50 different noise sequences.

- triggered frequency and voltage control of ac microgrids," *IEEE Trans. Power Systems*, vol. 37, no. 3, pp. 1979–1994, May 2022.
- [11] S. Abhinav, I. D. Schizas, F. Ferrese, and A. Davoudi, "Optimization-based ac microgrid synchronization," *IEEE Trans. Industrial Informatics*, vol. 13, no. 5, pp. 2339–2349, Oct. 2017.
- [12] A. Bidram, F. L. Lewis, and A. Davoudi, "Distributed control systems for small-scale power networks: Using multiagent cooperative control theory," *IEEE Control Systems Magazine*, vol. 34, no. 6, pp. 56–77, Dec. 2014.
- [13] R. de Azevedo, M. H. Cintuglu, T. Ma, and O. A. Mohammed, "Multiagent-based optimal microgrid control using fully distributed diffusion strategy," *IEEE Trans. Smart Grid*, vol. 8, no. 4, pp. 1997– 2008, July. 2017.
- [14] N. M. Dehkordi and S. Z. Moussavi, "Distributed resilient adaptive control of islanded microgrids under sensor/actuator faults," *IEEE Trans. Smart Grid*, vol. 11, no. 3, pp. 2699–2708, May. 2020.
- [15] Y. Wang, T. L. Nguyen, M. H. Syed, Y. Xu, E. Guillo-Sansano, V.-H. Nguyen, G. M. Burt, Q.-T. Tran, and R. Caire, "A distributed control scheme of microgrids in energy internet paradigm and its multisite implementation," *IEEE Trans. Industrial Informatics*, vol. 17, no. 2, pp. 1141–1153, Feb. 2021.
- [16] Y. Hong, G. Chen, and L. Bushnell, "Distributed observers design for leader-following control of multi-agent networks," *Automatica*, vol. 44, no. 3, pp. 846–850, Mar. 2008.
- [17] J. Hu and G. Feng, "Distributed tracking control of leader-follower multi-agent systems under noisy measurement," *Automatica*, vol. 46, no. 8, pp. 1382–1387, August. 2010.
- [18] Y. Pang, H. Xia, and M. J. Grimble, "Resilient nonlinear control for attacked cyber-physical systems," *IEEE Trans. Systems, Man, and Cybernetics: Systems*, vol. 50, no. 6, pp. 2129–2138, Mar. 2018.
- [19] N. M. Dehkordi, H. R. Baghaee, N. Sadati, and J. M. Guerrero, "Distributed noise-resilient secondary voltage and frequency control for islanded microgrids," *IEEE Trans. Smart Grid*, vol. 10, no. 4, pp. 3780– 3790, May. 2018.
- [20] N. M. Dehkordi and V. Nekoukar, "Robust distributed stochastic secondary control of microgrids with system and communication noises," *IET Generation, Transmission, & Distribution*, vol. 14, no. 6, pp. 1148– 1158, Mar. 2020.
- [21] S. Abhinav, I. D. Schizas, and A. Davoudi, "Noise-resilient synchrony of ac microgrids," in 2015 Resilience Week (RWS). IEEE, Aug. 2015, pp. 1–6.
- [22] S. Abhinav, I. D. Schizas, F. L. Lewis, and A. Davoudi, "Distributed

- noise-resilient networked synchrony of active distribution systems," *IEEE Trans. Smart Grid*, vol. 9, no. 2, pp. 836–846, May. 2016.
- [23] S. Shrivastava, B. Subudhi, and S. Das, "Noise-resilient voltage and frequency synchronisation of an autonomous microgrid," *IET Generation*, *Transmission & Distribution*, vol. 13, no. 2, pp. 189–200, Dec. 2019.
- [24] R. Bhattarai, N. Gurung, and S. Kamalasadan, "Dual mode control of a three-phase inverter using minimum variance adaptive architecture," *IEEE Trans. Industry Applications*, vol. 54, no. 4, pp. 3868–3880, Apr. 2018.
- [25] F. Chen, M. Chen, Z. Xu, J. M. Guerrero et al., "Distributed noise-resilient economic dispatch strategy for islanded microgrids," *IET Generation, Transmission & Distribution*, vol. 13, no. 14, pp. 3029–3039, June. 2019.
- [26] J. Lai, X. Lu, X. Yu, W. Yao, J. Wen, and S. Cheng, "Noise-resilient distributed frequency control for droop-controlled renewable microgrids," in 2018 13th IEEE conference on industrial electronics and applications (ICIEA). IEEE, May. 2018, pp. 1244–1249.
- [27] M. Amini, A. I. Sarwat, S. Iyengar, and I. Guvenc, "Determination of the minimum-variance unbiased estimator for dc power-flow estimation," in IECON 2014-40th Annual Conference of the IEEE Industrial Electronics Society. IEEE, Oct. 2014, pp. 114–118.
- [28] L. Cheng, Z.-G. Hou, and M. Tan, "A mean square consensus protocol for linear multi-agent systems with communication noises and fixed topologies," *IEEE Trans. Automatic Control*, vol. 59, no. 1, pp. 261– 267, June. 2013.

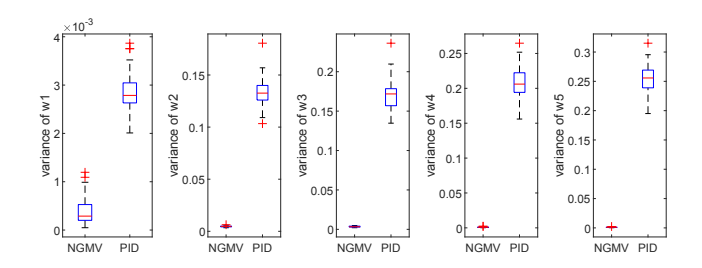


Fig. 29. Comparison of the variance of noise on DG1's to DG5's frequencies in Microgrid test system II for 50 different noise sequences.

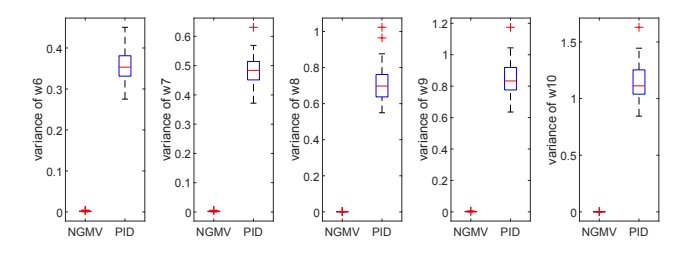


Fig. 30. Comparison of the variance of noise on DG6's to DG10's frequencies in Microgrid test system II for 50 different noise sequences.

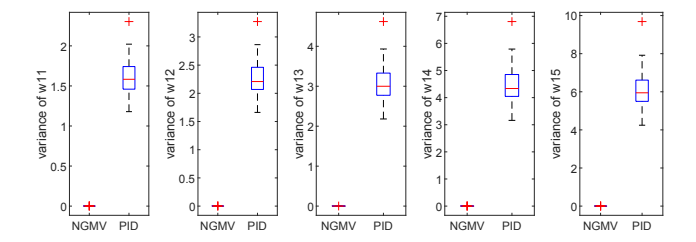


Fig. 31. Comparison of the variance of noise on DG11's to DG15's frequencies in Microgrid test system II for 50 different noise sequences.

- [29] R. W. Brockett, "Volterra series and geometric control theory," *Automatica*, vol. 12, no. 2, pp. 167–176, 1976.
- [30] F. J. Doyle III, B. A. Ogunnaike, and R. K. Pearson, "Nonlinear model-based control using second-order volterra models," *Automatica*, vol. 31, no. 5, pp. 697–714, 1995.
- [31] F. J. Doyle, R. K. Pearson, and B. A. Ogunnaike, *Identification and control using Volterra models*. Springer, 2002.
- [32] L. Lu, X. Yang, W. Wang, and Y. Yu, "Recursive second-order volterra filter based on dawson function for chaotic memristor system identification," *Nonlinear Dynamics*, vol. 99, no. 4, pp. 3123–3142, Jan. 2020.
- [33] C. Cheng, Z. Peng, W. Zhang, and G. Meng, "Volterra-series-based nonlinear system modeling and its engineering applications: A stateof-the-art review," *Mechanical Systems and Signal Processing*, vol. 87, pp. 340–364, 2017.
- [34] M. J. Grimble, "Non-linear generalized minimum variance feedback, feedforward and tracking control," *Automatica*, vol. 41, no. 6, pp. 957– 969, June. 2005.
- [35] M. Kazemi, M. M. Arefi, and Y. Alipouri, "Wiener model based gmvc design considering sensor noise and delay," *ISA Transactions*, vol. 88, pp. 73–81, May. 2019.
- [36] M. Maboodi, A. Khaki-Sedigh, and E. F. Camacho, "Control performance assessment for a class of nonlinear systems using second-order volterra series models based on nonlinear generalised minimum variance control," *International Journal of Control*, vol. 88, no. 8, pp. 1565–1575, Feb. 2015.
- [37] O. Nelles, Nonlinear system identification: from classical approaches to neural networks, fuzzy models, and gaussian processes. Springer Nature. 2020.
- [38] Z. Zhang and J. Chen, "Enhancing performance of generalized minimum variance control via dynamic data reconciliation," *Journal of the Franklin Institute*, vol. 356, no. 15, pp. 8829–8854, Oct. 2019.
- [39] M. A. Sheikhi, A. Khaki-Sedigh, and A. Nikoofard, "Design of nonlinear predictive generalized minimum variance control for performance monitoring of nonlinear control systems," *Journal of Process Control*, vol. 106, pp. 54–71, Oct. 2021.
- [40] S. Boyd, S. P. Boyd, and L. Vandenberghe, Convex optimization. Cambridge university press, 2004.
- [41] L. T. Biegler, Nonlinear programming: concepts, algorithms, and applications to chemical processes. SIAM, 2010.

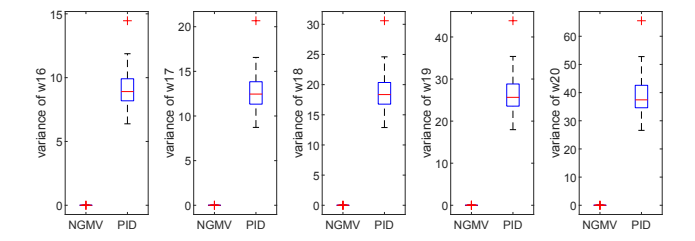


Fig. 32. Comparison of the variance of noise on DG16's to DG20's frequencies in Microgrid test system II for 50 different noise sequences.